Scaling of forced magnetic reconnection in the Hall-magnetohydrodynamic Taylor problem

Richard Fitzpatrick

Citation: Physics of Plasmas (1994-present) **11**, 937 (2004); doi: 10.1063/1.1640378
View online: http://dx.doi.org/10.1063/1.1640378
View Table of Contents: http://scitation.aip.org/content/aip/journal/pop/11/3?ver=pdfcov
Published by the AIP Publishing

Scaling of forced magnetic reconnection in the Hall-magnetohydrodynamic Taylor problem

Richard Fitzpatrick[a)]
Center for Magnetic Reconnection Studies, Institute for Fusion Studies, Department of Physics, University of Texas at Austin, Austin, Texas 78712

(Received 15 July 2003; accepted 17 November 2003)

Two-dimensional, incompressible, zero guide-field, nonlinear Hall-MHD (magnetohydrodynamical) simulations are used to investigate the scaling of the rate of forced magnetic reconnection in the so-called Taylor problem. In this problem, a small-amplitude boundary perturbation is suddenly applied to a tearing stable, slab plasma equilibrium; the perturbation being such as to drive magnetic reconnection within the plasma. This type of reconnection, which is not due to an intrinsic plasma instability, is generally known as ''forced reconnection.'' The inclusion of the Hall term in the plasma Ohm's law is found to greatly accelerate the rate of magnetic reconnection. In the linear Hall-MHD regime, the peak instantaneous reconnection rate is found to scale like $d\Psi/dt \sim d_i \eta^{1/3} \Xi_0$, where Ψ is the reconnected magnetic flux, d_i the collisionless ion skin depth, η the resistivity, and Ξ_0 the amplitude of the boundary perturbation. In the nonlinear Hall-MHD regime, the peak reconnection rate is found to scale like $d\Psi/dt \sim d_i^{3/2} \Xi_0^2$. © *2004 American Institute of Physics.* [DOI: 10.1063/1.1640378]

I. INTRODUCTION

Magnetic reconnection is a phenomenon that occurs in a wide variety of laboratory and space plasmas: e.g., magnetic fusion experiments,[1] the solar corona,[2] and the Earth's magnetotail.[3] The reconnection process gives rise to changes in magnetic field-line topology with an accompanying transformation of magnetic energy into particle energy. Conventional single-fluid resistive magnetohydrodynamical (MHD) theory is capable of accounting for magnetic reconnection, but generally predicts reconnection rates that are many orders of magnitude smaller than those observed.[4] More sophisticated plasma models that treat electrons and ions as separate fluids yield much faster reconnection rates that are more consistent with observations.[5,6]

This paper investigates a particular two-dimensional (2-D) magnetic reconnection problem that was first proposed by J. B. Taylor. In this problem, a high-β, stable, slab plasma equilibrium with a central magnetic field null is subject to a suddenly imposed, small-amplitude boundary perturbation that is such as to drive magnetic reconnection at the null. This type of reconnection, which is not due to an intrinsic plasma instability, is generally termed ''forced reconnection.'' The so-called ''Taylor problem'' has already been thoroughly investigated within the context of conventional resistive MHD.[7,8] The aim of this paper is to extend this investigation so as to take two-fluid effects into account. Unfortunately, the inclusion of two-fluid effects complicates the problem sufficiently that it is no longer amenable to an analytic treatment. Hence, in this paper our investigation is limited to scaling studies performed by means of numerical simulations.

In conventional MHD theory, the electron and ion fluids are constrained to move together as a single fluid. For a sufficiently collisional plasma this is indeed a correct description of the plasma dynamics. However, the plasmas encountered in astrophysical, space, and magnetic fusion contexts are generally not collisional enough for conventional MHD to remain a valid model. Now, in less collisional plasmas, the ion and electron fluids decouple on length scales below the *collisionless ion skin depth*, $d_i = c/\omega_{pi}$.[9] This decoupling of the ion and electron fluids is effected by the so-called Hall term in the plasma Ohm's law. Furthermore, the electron fluid decouples from the magnetic field on length scales below the *collisionless electron skin depth*, $d_e = c/\omega_{pe} \ll d_i$. This decoupling of the electron fluid and the magnetic field is affected by the electron inertia term in the plasma Ohm's law. In this paper, we shall investigate the Taylor problem using a so-called ''Hall-MHD'' model in which the width, δ, of the reconnecting region is determined by *resistivity*, and is such that $d_e \ll \delta \lesssim d_i$. It follows that we shall include the Hall term in our plasma Ohm's law but neglect electron inertia. Obviously, the Hall-MHD model is only valid for plasmas that are sufficiently collisional that $\delta \gg d_e$. Fortunately, this is a far less onerous constraint than that which must be satisfied by the conventional MHD model: i.e., $\delta \gg d_i$.

II. PRELIMINARY ANALYSIS

A. Basic equations

Standard right-handed Cartesian coordinates (x,y,z) are adopted. It is assumed that there is no variation along the z axis: i.e., $\partial/\partial z \equiv 0$. Consider an incompressible, magnetized, two-species (electron and ion), quasineutral plasma with singly charged ions that is governed by fluid equations. Let the

a)Electronic mail: rfitzp@farside.ph.utexas.edu

ion/electron number density, n, the resistivity, η, and the ion/electron viscosity, $\mu_{i,e}$, be uniform. We can write[10]

$$nm_e\left[\frac{\partial \mathbf{V}_e}{\partial t}+(\mathbf{V}_e\cdot\nabla)\mathbf{V}_e\right]=-\nabla p_e-ne(\mathbf{E}+\mathbf{V}_e\wedge\mathbf{B})+\mu_e\nabla^2\mathbf{V}_e+ne\,\eta\mathbf{j}, \tag{1}$$

$$nm_i\left[\frac{\partial \mathbf{V}_i}{\partial t}+(\mathbf{V}_i\cdot\nabla)\mathbf{V}_i\right]=-\nabla p_i+ne(\mathbf{E}+\mathbf{V}_i\wedge\mathbf{B})+\mu_i\nabla^2\mathbf{V}_i-ne\,\eta\mathbf{j}, \tag{2}$$

where $\mathbf{E}$ is the electric field-strength, $\mathbf{B}$ the magnetic field-strength, $\mathbf{j}$ the current density, $m_{i,e}$ the ion/electron mass, $\mathbf{V}_{i,e}$ the ion/electron velocity, and $p_{i,e}$ the ion/electron pressure. We can also write

$$\nabla\cdot\mathbf{V}_{i,e}=0, \tag{3}$$

$$ne(\mathbf{V}_i-\mathbf{V}_e)=\mathbf{j}. \tag{4}$$

Finally, Maxwell's equations yield

$$\nabla\cdot\mathbf{B}=0, \tag{5}$$

$$\nabla\wedge\mathbf{B}=\mu_0\mathbf{j}, \tag{6}$$

$$\nabla\wedge\mathbf{E}=-\frac{\partial\mathbf{B}}{\partial t}. \tag{7}$$

B. Normalization

Let $\hat{\nabla}=a\nabla$, $\hat{t}=t/(a/V_{\rm A})$, $\hat{\mathbf{B}}=\mathbf{B}/B_0$, $\hat{\mathbf{E}}=\mathbf{E}/(B_0V_{\rm A})$, $\hat{\mathbf{j}}=\mathbf{j}/[B_0/(\mu_0 a)]$, $\hat{\mathbf{V}}_{i,e}=\mathbf{V}_{i,e}/V_{\rm A}$, $\hat{p}_{i,e}=p_{i,e}/(B_0^2/\mu_0)$, $\hat{\eta}=\eta/(\mu_0V_{\rm A}a)$, $\hat{\mu}_{i,e}=\mu_{i,e}/(V_{\rm A}anm_i)$, where a is a typical length scale, B_0 a typical magnetic field-strength, and $V_{\rm A}=B_0/\sqrt{\mu_0 nm_i}$ is a typical Alfvén speed. The normalized versions of Eqs. (1)–(7) take the form

$$\epsilon d_i\left[\frac{\partial \mathbf{V}_e}{\partial t}+(\mathbf{V}_e\cdot\nabla)\mathbf{V}_e\right]=-d_i\nabla p_e-(\mathbf{E}+\mathbf{V}_e\wedge\mathbf{B})+\epsilon d_i\mu_e\nabla^2\mathbf{V}_e+\eta\mathbf{j}, \tag{8}$$

$$d_i\left[\frac{\partial \mathbf{V}_i}{\partial t}+(\mathbf{V}_i\cdot\nabla)\mathbf{V}_i\right]=-d_i\nabla p_i+(\mathbf{E}+\mathbf{V}_i\wedge\mathbf{B})+d_i\mu_i\nabla^2\mathbf{V}_i-\eta\mathbf{j}, \tag{9}$$

$$\nabla\cdot\mathbf{V}_{i,e}=0, \tag{10}$$

$$\mathbf{V}_i-\mathbf{V}_e=d_i\mathbf{j}, \tag{11}$$

$$\nabla\cdot\mathbf{B}=0, \tag{12}$$

$$\nabla\wedge\mathbf{B}=\mathbf{j}, \tag{13}$$

$$\nabla\wedge\mathbf{E}=-\frac{\partial\mathbf{B}}{\partial t}, \tag{14}$$

where all over carets have been neglected for ease of notation. Here, $\epsilon=m_e/m_i$ is the electron–ion mass ratio, whereas $d_i=(c/\omega_{pi})/a$ is the normalized *collisionless ion skin depth*, with $\omega_{pi}=\sqrt{ne^2/\epsilon_0 m_i}$.

Neglecting electron inertia (i.e., letting $\epsilon\rightarrow 0$), Eqs. (8) and (9) can be combined to give an *ion equation of motion*,

$$\frac{\partial \mathbf{V}_i}{\partial t}+(\mathbf{V}_i\cdot\nabla)\mathbf{V}_i=-\nabla(p_i+p_e)+\mathbf{j}\wedge\mathbf{B}+\mu_i\nabla^2\mathbf{V}_i, \tag{15}$$

and a *generalized Ohm's law*,

$$\mathbf{E}+\mathbf{V}\wedge\mathbf{B}=\eta\mathbf{j}+d_i\mathbf{j}\wedge\mathbf{B}-d_i\nabla p_e-\nu\nabla^2\mathbf{j}. \tag{16}$$

Equation (15) is fairly standard. However, Eq. (16) contains a pair of terms that do not occur in conventional MHD. Namely, the second and third terms on the right-hand side, which are usually called the *Hall* and *electron pressure* terms, respectively. The final term on the right-hand side of Eq. (16) (which is added for numerical reasons) corresponds to a phenomenological *hyper-resistivity*. This term might arise from an anomalously large electron viscosity, or alternatively via the braiding of magnetic field lines. The hyper-resistivity parameter, ν, is assumed to be uniform.

C. Normalized equations

Without loss of generality, we can write

$$\mathbf{B}=\nabla\psi\wedge\hat{\mathbf{z}}+B_z\hat{\mathbf{z}}, \tag{17}$$

$$\mathbf{V}_i=\nabla\phi\wedge\hat{\mathbf{z}}+V_z\hat{\mathbf{z}}, \tag{18}$$

and $E_z=-\partial\psi/\partial t$. After some manipulation, our normalized equations reduce to

$$\frac{\partial\psi}{\partial t}=[\phi,\psi]+d_i[\psi,B_z]+\eta\nabla^2\psi-\nu\nabla^4\psi, \tag{19}$$

$$\frac{\partial B_z}{\partial t}=[\phi,B_z]+[V_z,\psi]+d_i[\psi,j_z]+\eta\nabla^2B_z-\nu\nabla^4B_z, \tag{20}$$

$$\frac{\partial\omega_z}{\partial t}=[\phi,\omega_z]+[j_z,\psi]+\mu_i\nabla^2\omega_z, \tag{21}$$

$$\frac{\partial V_z}{\partial t}=[\phi,V_z]+[B_z,\psi]+\mu_i\nabla^2V_z, \tag{22}$$

where

$$j_z=-\nabla^2\psi \tag{23}$$

$$\omega_z=-\nabla^2\phi, \tag{24}$$

$$[A,B]\equiv\nabla A\wedge\nabla B\cdot\hat{\mathbf{z}}. \tag{25}$$

D. Plasma equilibrium

Suppose that the plasma is bounded by perfectly conducting walls located at $x=\pm 1$, and is periodic in the y direction with periodicity length L. The initial plasma equilibrium satisfies

$$\psi^{(0)}(x)=-\frac{x^2}{2}, \tag{26}$$

and $B_z^{(0)}(x)=\phi^{(0)}(x)=V_z^{(0)}(x)=0$. Note that $j_z^{(0)}(x)=1$ and $\omega_z^{(0)}(x)=0$. In unnormalized units, B_0 is the equilibrium magnetic field strength at $|x|=a$, and a is half the distance between the conducting walls. Note that the above plasma equilibrium is *completely stable* to tearing modes.

E. Boundary conditions

Suppose that the conducting wall at $x=1$ is subject to a *small* (compared with unity) displacement $\Xi(t)\sin(ky)$ in the x direction, where $k=2\pi/L$. An equal and opposite displacement is applied to the wall at $x=-1$. The appropriate boundary conditions at the walls are

$$\psi(\pm 1,y,t)=-\tfrac{1}{2}+\Xi(t)\sin(ky), \tag{27}$$

$$B_z(\pm 1,y,t)=0, \tag{28}$$

$$\phi(\pm 1,y,t)=\mp\frac{1}{k}\frac{d\Xi(t)}{dt}\cos(ky), \tag{29}$$

$$\omega_z(\pm 1,y,t)=0, \tag{30}$$

$$V_z(\pm 1,y,t)=0. \tag{31}$$

Let

$$\Xi(t)=\Xi_0[1-e^{-t/\tau}-(t/\tau)e^{-t/\tau}], \tag{32}$$

for $t\geqslant 0$, with $\Xi(t)=0$ for $t<0$. Note that both $\Xi(t)$ and $d\Xi(t)/dt$ are continuous at $t=0$, and $\Xi(t)\rightarrow\Xi_0$ as $t\rightarrow\infty$. All fields are assumed to be unperturbed at $t=0$.

F. Reconnection diagnostics

The magnetic O and X points are located at $(x,y)=(0,L/4)$ and $(0,3L/4)$, respectively. The *reconnected magnetic flux* is written as

$$\Psi(t)=\tfrac{1}{2}[\psi(\text{X point})-\psi(\text{O point})]. \tag{33}$$

It is helpful to define the *normalized magnetic reconnection rate*,

$$J(t)=\eta^{-1}\frac{d\Psi(t)}{dt}. \tag{34}$$

It follows from Eqs. (19)–(24) and via symmetry that

$$J(t)=\frac{1}{2}[j_z(\text{O point})-j_z(\text{X point})]+\frac{\nu}{\eta}\frac{1}{2}[\nabla^2 j_z(\text{X point})-\nabla^2 j_z(\text{O point})]. \tag{35}$$

G. Discussion

Equations (19)–(24) represent the simplest system of equations that permit an investigation of the effect of the Hall term on the rate of 2-D magnetic reconnection in the absence of a strong guide field (i.e., a strong equilibrium B_z). Note that in the limit $d_i\rightarrow 0$ (i.e., the limit in which the collisionless ion skin depth, c/ω_{pi}, becomes much smaller than a typical variation length scale) our system of equations reverts to conventional MHD. In the following, we review the many assumptions made during the derivation of Eqs. (19)–(24).

We have adopted a fluid description of the electron and ion motion: i.e., Eqs. (1) and (2). Also, for the sake of simplicity, we have used isotropic pressure, resistivity, and viscosity operators. These choices exclude potentially important kinetic and finite Larmor radius effects from our model. However, Birn *et al.* (2001)[11] have demonstrated that a fluid approach to 2-D Hall-MHD magnetic reconnection in the absence of a guide field generates virtually identical reconnection rates to more sophisticated particle approaches that include kinetic and finite Larmor radius effects.

We have assumed that both the electron and ion fluids are *incompressible*. According to Biskamp *et al.* (1997),[12] this assumption is justified for Hall reconnection in the *absence* of a strong guide field. Note, incidentally, that the electron pressure term in the generalized Ohm's law (16) makes *no contribution* to Eqs. (19)–(24) in the incompressible limit.

We have neglected electron inertia effects. This neglect is justified provided that the length scales of interest in our problem remain significantly larger than the collisionless electron skin depth, c/ω_{pe}. This condition is easily satisfied in our simulations.

We have added a phenomenological hyper-resistivity term to our generalized Ohm's law (16). In order to appreciate the need for such a term, consider the following whistler wave dispersion relation, which is obtained from Eqs. (19)–(24), in the limit $d_i\gg 1$, assuming an $e^{i(k_y y-\omega t)}$ dependence of perturbed quantities:

$$\omega\simeq d_i x k_y^2-i\eta k_y^2-i\nu k_y^4. \tag{36}$$

Note that the whistler wave propagates with a phase velocity that *increases* with decreasing wavelength, but is damped by both resistivity and hyper-resistivity. Note also that resistivity alone is incapable of effectively damping short wavelength whistler waves, since the first two terms on the right-hand side of the above equation both scale like k_y^2. On the other hand, the hyper-resistivity term, which scales like k_y^4, is quite capable of damping short wavelength modes. Not surprisingly, therefore, in the absence of hyper-resistivity there is a collapse to short wavelength modes, in the nonlinear Hall-MHD regime, which poses severe numerical difficulties. Hyper-resistivity halts this collapse before it becomes problematic.[11,13] Note that the magnetic reconnection rate in the nonlinear Hall-MHD regime is almost independent of the value of ν (provided that ν is sufficiently large to prevent scale collapse).

III. NUMERICAL RESULTS

A. Introduction

Equations (19)–(24), plus the initial equilibrium described in Sec. II D and the boundary conditions (27)–(32), have been implemented numerically in a finite-difference code that is second-order in both space and time. The code makes use of a semi-implicit algorithm modeled after that of Harned and Mikic[14] in order to circumvent the highly restrictive Courant–Freidrichs–Lewy condition on the whistler wave. The computational grid is uniform in the y direction. However, in order to help resolve the reconnecting region, the grid points in the x direction are more closely packed in the vicinity of the magnetic resonance. All of the simulations

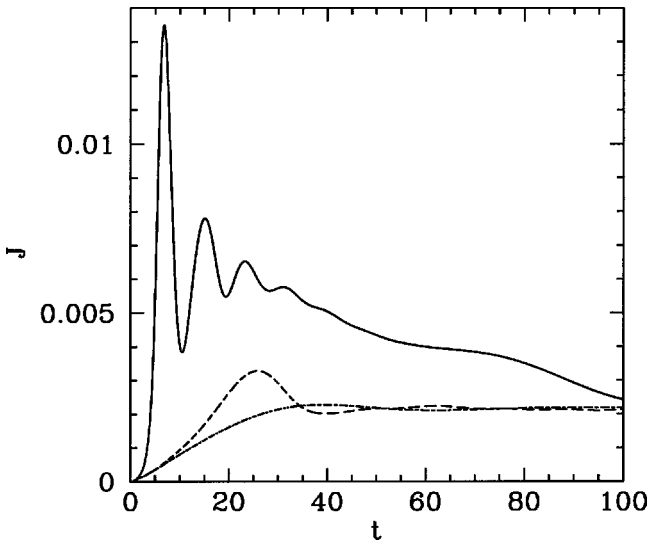

FIG. 1. The magnetic reconnection rate, J, versus time for various values of the collisionless ion skin depth, d_i. Calculations performed with $L=8.0$, $\tau=1.0$, $\eta=10^{-4}$, $\mu_i=10^{-8}$, $\nu=0.0$, and $\Xi_0=10^{-4}$. The dotted–dashed curve corresponds to $d_i=0.0$. The dashed curve corresponds to $d_i=0.1$. The solid curve corresponds to $d_i=1.0$. The maximum J values are 2.284×10^{-3}, 3.285×10^{-3}, and 1.354×10^{-2}, respectively. The reconnected fluxes, ψ, at $t=100$ are 1.877×10^{-5}, 2.044×10^{-5}, and 4.544×10^{-5}, respectively.

discussed in this paper employ a uniform time step of $\delta t=10^{-3}$ normalized time units, as well as a 256×128 computational grid.

B. Overview

Figure 1 shows the time variation of the magnetic reconnection rate, J, calculated for three different values of the collisionless ion skin depth, d_i, with all other parameters held constant. Note that in all three cases the amplitude of the applied perturbation is sufficiently low that the reconnection takes place in the *linear* regime.

The case $d_i=0$ corresponds to conventional MHD. In this limit, the rate of forced reconnection is well described by the analysis of Hahm and Kulsrud,[7] which was recently verified via numerical simulation.[8] According to this analysis, the reconnection takes place in two main phases. In the first phase, the plasma response is dominated by *ion inertia*, with resistivity and viscosity playing negligible roles. Now, the plasma response to the wall perturbation is governed by the well-known equations of marginally stable, ideal MHD everywhere apart from a thin layer, centered on the resonant surface ($x=0$), in which a strong current is driven. In the inertial regime, this layer is of thickness $\delta\sim t^{-1}$. The reconnection rate in the inertial regime varies like $J\propto t\Xi_0$. Finally, the inertial regime ends when $t\rightarrow\tau_1$, where $\tau_1=\eta^{-1/3}$. For $t\gg\tau_1$, the plasma response is governed by standard constant-ψ layer physics.[15] In the constant-ψ regime, the reconnection rate decays on a typical tearing time scale (which is much longer than τ_1), and the width of the current layer gradually increases. The reconnection rate peaks around the time, $t\sim\tau_1$, at which the plasma response makes the transition from the inertial regime to the constant-ψ regime. The peak magnetic reconnection rate takes the form

$$J_{\max}\sim\eta^{-1/3}\Xi_0. \tag{37}$$

The minimum width of the current layer (which also occurs around $t\sim\tau_1$) is

$$\delta_{\min}\sim\eta^{1/3}. \tag{38}$$

It can be seen from Fig. 1 that the Hall term, which is parametrized by d_i, *greatly accelerates* the rate of forced magnetic reconnection. Indeed, as d_i becomes larger, the peak reconnection rate both increases in magnitude and occurs at earlier and earlier times. A similar significant acceleration in the rate of magnetic reconnection due to the inclusion of the Hall term in Ohm's law has been reported in earlier studies.[16,17]

Figure 2 compares and contrasts the current density, j_z, out-of-plane magnetic field, B_z, and ion streamfunction, ϕ, patterns calculated at the time of the peak reconnection rate for a typical *linear* MHD simulation ($d_i=10^{-3}$) and a typical *linear* Hall-MHD simulation ($d_i=1.0$). It can be seen that the reconnecting layer, within which the current density is strongly peaked, is significantly thinner in the Hall-MHD simulation. Moreover, there is far less structure outside the layer in the Hall-MHD simulation. However, the main difference between the two simulations lies in the fact that in the Hall-MHD simulation the ion motion is clearly *completely decoupled* from the reconnecting layer. On the other hand, the ion motion is strongly coupled to the reconnecting layer in the conventional MHD simulation. This effect takes place because in Hall-MHD the ion and electron motions decouple on length scales below the collisionless ion skin depth, d_i.[9,16] It follows that in the Hall-MHD regime (in which the width of the reconnecting layer is much less than d_i) the current in the reconnecting layer is carried almost entirely by electrons.

Figure 3 compares and contrasts the current density, j_z, out-of-plane magnetic field, B_z, and ion streamfunction, ϕ, patterns calculated at the time of the peak reconnection rate for a typical *nonlinear* MHD simulation ($d_i=10^{-3}$) and a typical *nonlinear* Hall-MHD simulation ($d_i=1.0$). The conventional MHD simulation exhibits the extended narrow current sheet that is characteristic of Sweet–Parker magnetic reconnection.[1,18,19] Note, in particular, that the reconnected magnetic island does not extend over all values of y.[1] On the other hand, the Hall-MHD simulation is quite different. First, the current sheet is strongly concentrated around the X point, and is not particularly extended in the y direction.[16,20] Indeed, the current pattern is more reminiscent of Petschek reconnection[21] than Sweet–Parker reconnection. Note that the reconnected magnetic island now spans virtually all values of y. Second, the out-of-plane magnetic field is strongly localized in the vicinity of the island, and forms a characteristic quadrupole pattern around the X point.[22] Finally, as in the linear case, the ion motion is completely decoupled from the reconnecting region.

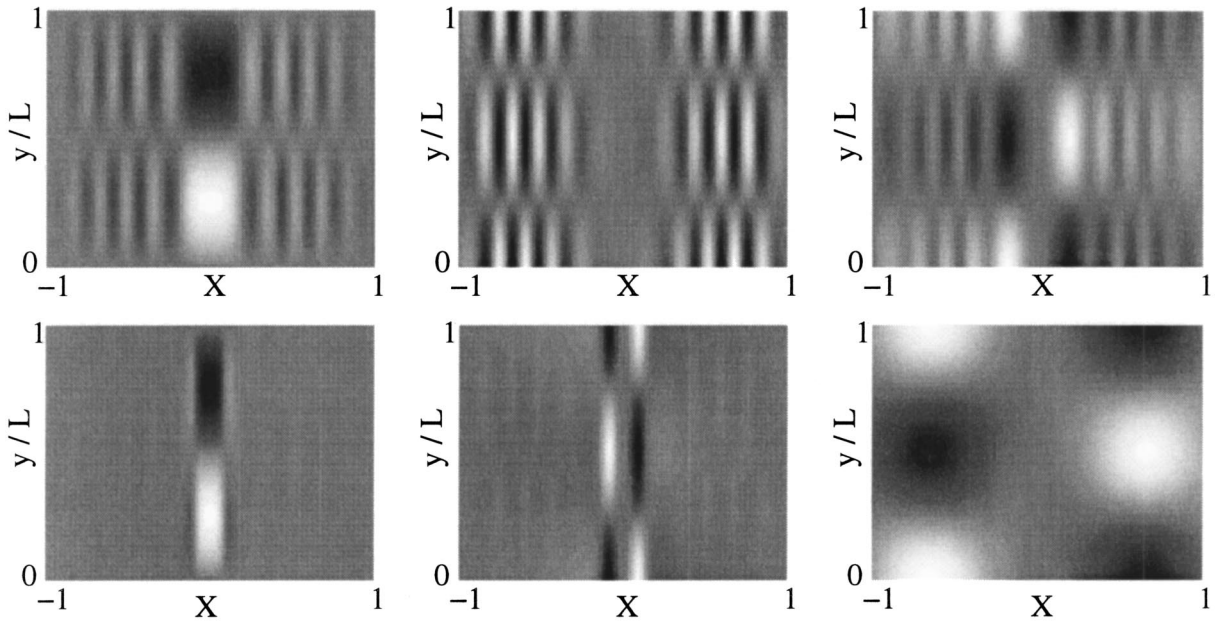

FIG. 2. Typical current density, etc., patterns associated with forced reconnection in the linear MHD and linear Hall-MHD regimes. Calculations performed with $L=8.0$, $\tau=1.0$, $\eta=10^{-4}$, $\mu_i=10^{-8}$, $\nu=0.0$, and $\Xi_0=10^{-4}$. All panels show data taken at the peak reconnection rate. The left panels show density plots of the current density, j_z. The middle panels show density plots of the out-of-plane magnetic field-strength, B_z. The right panels show density plots of the ion streamfunction, ϕ. The upper panels show calculations made using $d_i=10^{-3}$, corresponding to the linear MHD regime. The lower panels show calculations made using $d_i=1.0$, corresponding to the linear Hall-MHD regime. Note that $X=\mathrm{sgn}(x)\sqrt{|x|/(2-|x|)}$ is a stretched coordinate.

C. Scaling in the linear regime

Figure 4 shows the scaling of the peak magnetic reconnection rate, $J_{\max}$, with plasma resistivity, η, in the linear MHD and Hall-MHD regimes. As expected [see Eq. (37)], $J_{\max}$ scales as $\eta^{-1/3}$ in the linear MHD regime ($d_i=0.0$). This scaling breaks down at large η values because the width of the reconnecting layer (which scales as $\eta^{1/3}$) becomes too large for the asymptotic matching analysis of Hahm and

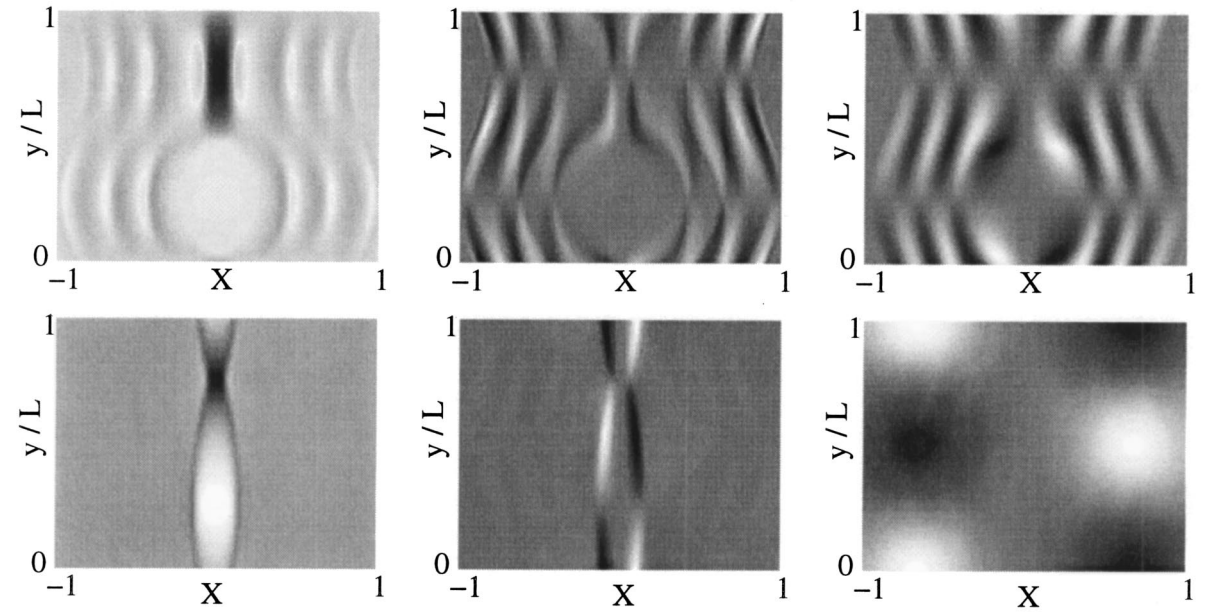

FIG. 3. Typical current density, etc., patterns associated with forced reconnection in the nonlinear MHD and nonlinear Hall-MHD regimes. Calculations performed with $L=8.0$, $\tau=1.0$, $\eta=10^{-5}$, and $\mu_i=10^{-6}$. All panels show data taken at the peak reconnection rate. The left panels show density plots of the current density, j_z. The middle panels show density plots of the out-of-plane magnetic field-strength, B_z. The right panels show density plots of the ion streamfunction, ϕ. The upper panels show calculations made using $d_i=10^{-3}$, $\nu=0.0$, and $\Xi_0=0.1$, corresponding to the nonlinear MHD regime. The lower panels show calculations made using $d_i=1.0$, $\nu=2.5\times10^{-9}$, and $\Xi_0=10^{-2}$, corresponding to the nonlinear Hall-MHD regime. Note that $X=\mathrm{sgn}(x)\sqrt{|x|/(2-|x|)}$ is a stretched coordinate.

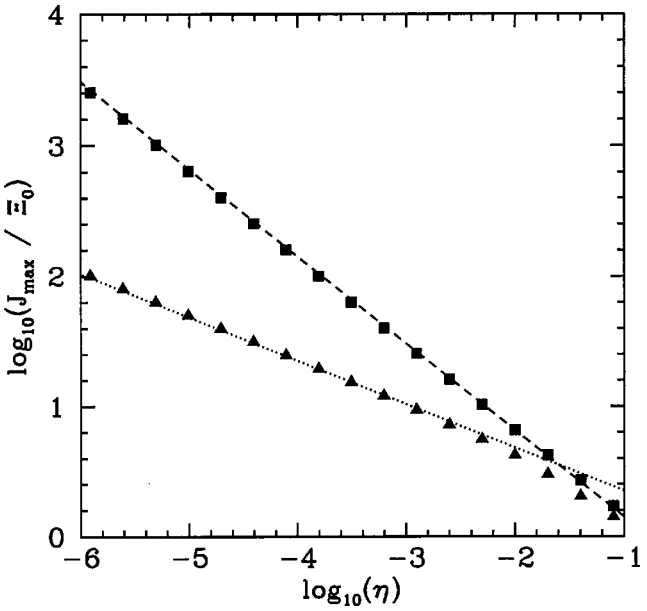

FIG. 4. Scaling of the peak magnetic reconnection rate, $J_{\max}$, with resistivity, η, in the linear regime. Zero hyper-resistivity calculations. Calculations performed with $L=8.0$, $\tau=1.0$, $\mu_i=0.0$, $\nu=0.0$, and $\Xi_0=10^{-4}$. The triangular data points correspond to $d_i=0.0$. The square data points correspond to $d_i=1.0$. The dashed line is a fit to $J_{\max}\propto\eta^{-2/3}$. The dotted line is a fit to $J_{\max}\propto\eta^{-1/3}$.

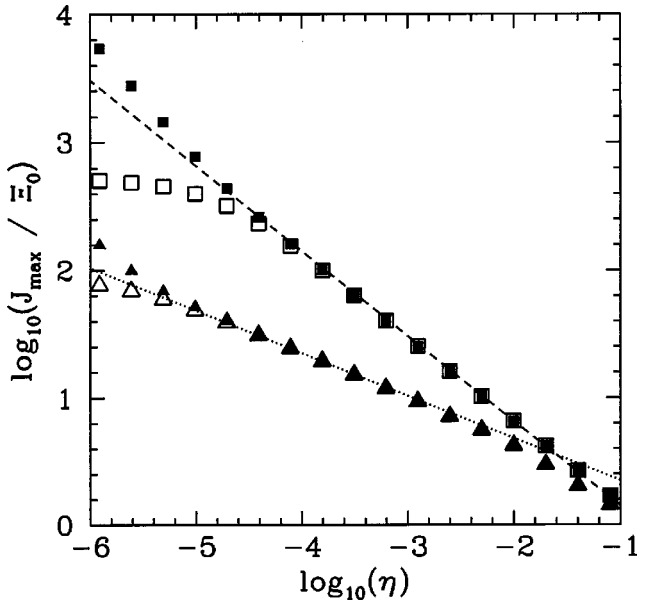

FIG. 5. Scaling of the peak magnetic reconnection rate, $J_{\max}$, with resistivity, η, in the linear regime. Finite hyper-resistivity calculations. Calculations performed with $L=8.0$, $\tau=1.0$, $\mu_i=0.0$, $\nu=2.5\times10^{-10}$, and $\Xi_0=10^{-4}$. The triangular data points correspond to $d_i=0.0$. The square data points correspond to $d_i=1.0$. The solid data points show the total reconnection rate. The open data points show the resistive contribution to the reconnection rate. The dashed line is a fit to $J_{\max}\propto\eta^{-2/3}$. The dotted line is a fit to $J_{\max}\propto\eta^{-1/3}$.

Kulsrud[7] to remain valid. On the other hand, $J_{\max}$ quite clearly scales as $\eta^{-2/3}$ in the linear Hall-MHD regime ($d_i=1.0$).

Figure 5 illustrates the effect of a small amount of hyper-resistivity on the resistive scaling of the peak magnetic reconnection rate in the linear MHD and Hall-MHD regimes. Now, in the presence of hyper-resistivity, there are two contributions to the reconnection rate—a resistive contribution and a hyper-resistive contribution, corresponding to the first and second term, respectively, on the right-hand side of Eq. (35). The resistive contribution to the reconnection rate is also equal to the amplitude of the current density perturbation in the reconnecting layer. It can be seen from Fig. 5 that at small η values the presence of finite hyper-resistivity leads to an *increase* (relative to the $\nu=0$ case) in the net reconnection rate, coupled with a corresponding *decrease* in the amplitude of the current density perturbation in the reconnecting layer (i.e., a decrease in the resistive contribution to the reconnection rate).

Figure 6 shows the scaling of the peak magnetic reconnection rate, $J_{\max}$, with the collisionless ion skin depth, d_i, in the linear regime. It can be seen that $J_{\max}$ is *independent* of d_i for d_i less than some critical value $(d_i)_{\rm crit}$. Of course, this limit corresponds to the conventional MHD regime. Note that $(d_i)_{\rm crit}$ clearly *increases* as η increases. When d_i exceeds $(d_i)_{\rm crit}$, and the Hall term in Ohm's law is thus able to affect reconnection, the peak reconnection rate starts to *increase* with increasing d_i.

Figure 7 is a rescaled version of Fig. 6. It is clear from Fig. 7 that

$$(d_i)_{\rm crit}\sim\eta^{1/3}. \tag{39}$$

Moreover, in the limit $(d_i)_{\rm crit}\ll d_i\ll 1$, there is good evidence from Fig. 7 for the following Hall-MHD scaling of $J_{\max}$:

$$J_{\max}\sim\frac{d_i}{\eta^{2/3}}\,\Xi_0. \tag{40}$$

Note, from Eq. (37), that the MHD scaling,

$$J_{\max}\sim\eta^{-1/3}\Xi_0, \tag{41}$$

holds for $d_i\ll(d_i)_{\rm crit}$. Finally, it is apparent from Fig. 6 that the increase in $J_{\max}$ with increasing d_i that is evident in Eq. (40) starts to level off as $d_i\to 1$ (i.e., as the collisionless ion skin depth becomes of the order the system size).

Now, a comparison of Eqs. (38) and (39) reveals that the plasma response enters the Hall-MHD regime when the collisionless ion skin depth, d_i, starts to *exceed* the width of the reconnecting layer. Of course, as soon as d_i becomes greater than the layer width, then the ion motion is able to decouple from the layer, which is the hallmark of Hall reconnection. Note that in the Hall-MHD regime the reconnecting layer width is always *much less* than d_i.

D. Scaling in the nonlinear MHD regime

In the nonlinear MHD regime we expect the reconnection to proceed according to the well-known Sweet–Parker scenario.[1,18,19] The appropriate scaling of $J_{\max}$ is[23]

$$J_{\max}\sim\frac{\Xi_0^{3/2}}{\eta^{1/2}}. \tag{42}$$

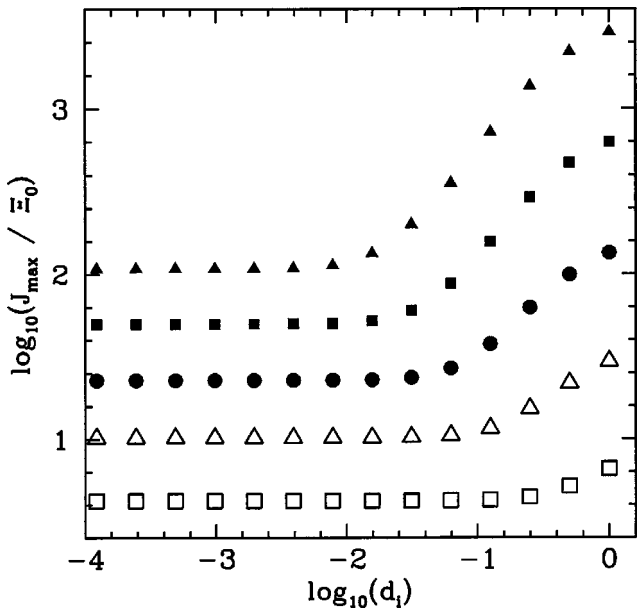

FIG. 6. Scaling of the peak magnetic reconnection rate, $J_{\max}$, with the collisionless ion skin depth, d_i, in the linear regime. Calculations performed with $L=8.0$, $\tau=1.0$, $\mu_i=0.0$, $\nu=0.0$, and $\Xi_0=10^{-4}$. The solid triangular data points correspond to $\eta=10^{-6}$. The solid square data points correspond to $\eta=10^{-5}$. The solid circular data points correspond to $\eta=10^{-4}$. The open triangular data points correspond to $\eta=10^{-3}$. The open square data points correspond to $\eta=10^{-2}$.

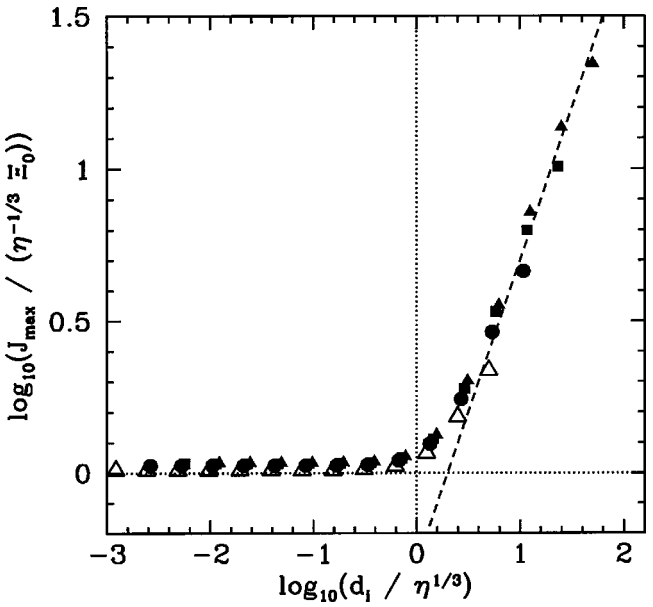

FIG. 7. Scaling of the normalized peak magnetic reconnection rate, $J_{\max}/\eta^{-1/3}$, with the normalized collisionless ion skin depth, $d_i/\eta^{1/3}$, in the linear regime. Calculations performed with $L=8.0$, $\tau=1.0$, $\mu_i=0.0$, $\nu=0.0$, and $\Xi_0=10^{-4}$. The solid triangular data points correspond to $\eta=10^{-6}$. The solid square data points correspond to $\eta=10^{-5}$. The solid circular data points correspond to $\eta=10^{-4}$. The open triangular data points correspond to $\eta=10^{-3}$. The dashed line is a fit to $J_{\max}/\eta^{-1/3}\propto d_i/\eta^{1/3}$.

Now, in Ref. 8, it was established that the plasma response enters the nonlinear regime when the perturbed current density in the reconnecting region becomes comparable to the local equilibrium current density. This implies that the criterion for nonlinearity is simply

$$J_{\max}\gtrsim 1 \tag{43}$$

(neglecting hyper-resistivity).

Figure 8 shows the scaling of the peak magnetic reconnection rate, $J_{\max}$, with resistivity, η, in the linear/nonlinear MHD regime. The expected $J_{\max}\sim\eta^{-1/2}$ scaling is obtained as long as $J_{\max}\gtrsim 1$: i.e., as long as the response is nonlinear.

Figure 9 shows the scaling of the peak magnetic reconnection rate, $J_{\max}$, with the wall perturbation amplitude, Ξ_0, in the linear/nonlinear MHD regime. It can be seen that for $J_{\max}\lesssim 1$ the linear scaling $J_{\max}\sim\Xi_0^1$ is obtained. However, for $J_{\max}\gtrsim 1$ we obtained the expected nonlinear scaling $J_{\max}\sim\Xi_0^{3/2}$.

Formula (42) is often thought of as pertaining only to *steady-state* reconnection. However, as is clear from the data shown in Figs. 8 and 9, this formula applies equally well to the type of *transient* forced reconnection obtained in the Taylor problem. The data shown in Figs. 8 and 9 also reinforces the observation, made in Ref. 8, that the plasma response enters the nonlinear regime when the current density perturbation in the reconnecting region becomes comparable to the local equilibrium current density (i.e., $J_{\max}\gtrsim 1$).

E. Scaling in the nonlinear Hall-MHD regime

Figure 10 shows the scaling of the peak magnetic reconnection rate, $J_{\max}$, with resistivity, η, in the linear/nonlinear Hall-MHD regime. The expected linear scaling $J_{\max}\sim\eta^{-2/3}$ [see Eq. (40)] is obtained when $J_{\max}\lesssim 1$. On the other hand, in the nonlinear regime (which corresponds to $J_{\max}\gtrsim 1$) we obtain the new scaling $J_{\max}\sim\eta^{-1}$. Note that in the nonlinear regime the hyper-resistive contribution to the reconnection rate dominates the resistive contribution. Moreover, as η decreases, the hyper-resistive contribution increases approxi-

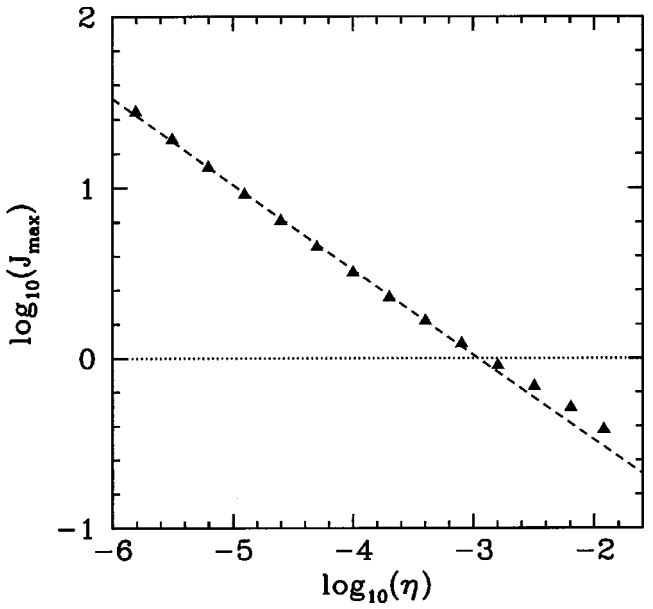

FIG. 8. Scaling of the peak magnetic reconnection rate, $J_{\max}$, with resistivity, η, in the linear/nonlinear MHD regime. Calculations performed with $L=8.0$, $\tau=1.0$, $\mu_i=\eta/10$, $\nu=0.0$, $d_i=0.0$, and $\Xi_0=0.1$. The dashed line is a fit to $J_{\max}\propto\eta^{-1/2}$.

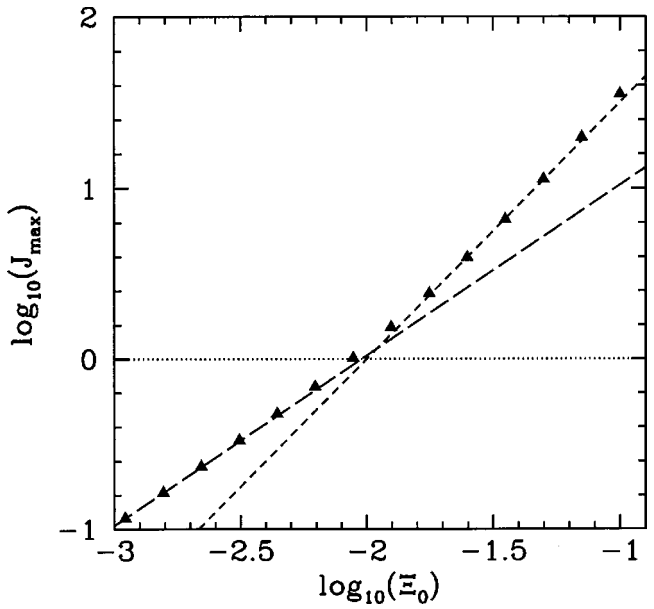

FIG. 9. Scaling of the peak magnetic reconnection rate, $J_{\max}$, with the perturbation amplitude, Ξ_0, in the linear/nonlinear MHD regime. Calculations performed with $L=8.0$, $\tau=1.0$, $\eta=10^{-6}$, $\mu_i=10^{-7}$, $\nu=0.0$, and $d_i=0.0$. The long-dashed line is a fit to $J_{\max}\propto\Xi_0^1$. The short-dashed line is a fit to $J_{\max}\propto\Xi_0^{3/2}$.

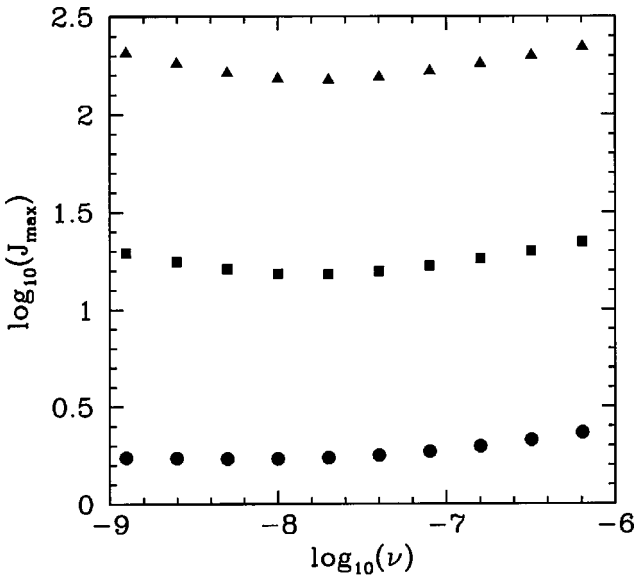

FIG. 11. Scaling of the peak magnetic reconnection rate, $J_{\max}$, with hyper-resistivity, ν, in the nonlinear Hall-MHD regime. Calculations performed with $L=8.0$, $\tau=1.0$, $\mu_i=\eta/10$, $d_i=1.0$, and $\Xi_0=10^{-2}$. The triangular data points show $\eta=10^{-6}$. The square data points show $\eta=10^{-5}$. The circular data points show $\eta=10^{-4}$.

mately as η^{-1}, whereas the resistive contribution (which also measures the amplitude of the perturbed current density in the reconnecting region) *saturates*.

Figure 11 shows the scaling of the peak magnetic reconnection rate, $J_{\max}$, with hyper-resistivity, ν, in the nonlinear Hall-MHD regime. It can be seen that the reconnection rate exhibits a fairly weak dependence on the hyper-resistivity.

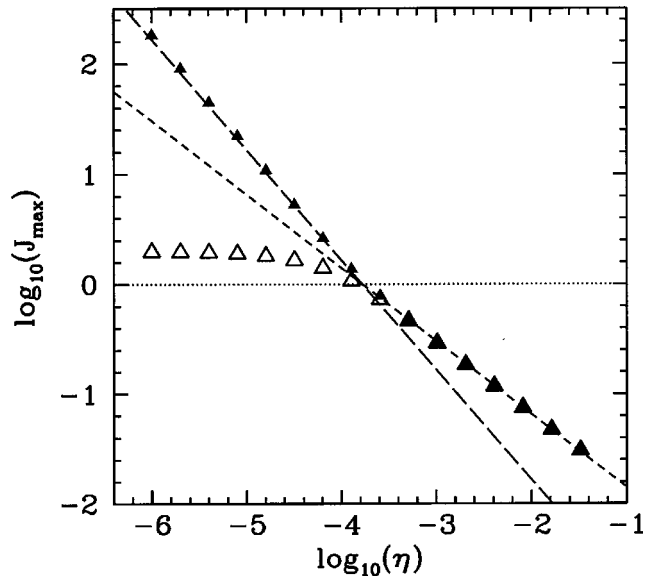

FIG. 10. Scaling of the peak magnetic reconnection rate, $J_{\max}$, with resistivity, η, in the linear/nonlinear Hall-MHD regime. Calculations performed with $L=8.0$, $\tau=1.0$, $\mu_i=\eta/10$, $\nu=2.5\times10^{-9}$, $d_i=1.0$, and $\Xi_0=10^{-2}$. The solid data points show the total reconnection rate. The open data points show the resistive contribution to the reconnection rate. The short-dashed line is a fit to $J_{\max}\propto\eta^{-2/3}$. The long-dashed line is a fit to $J_{\max}\propto\eta^{-1}$.

Now, magnetic reconnection implies a breakdown in both ion and electron *flux freezing*. In Hall-MHD, ion flux freezing breaks down automatically on length scales below d_i. However, electron flux freezing only breaks down in the reconnecting region due to the action of resistivity and hyper-resistivity. It is clear, from Figs. 10 and 11, that the peak rate of change of the reconnected magnetic flux, $(d\Psi/dt)_{\max}=\eta J_{\max}$, is virtually *independent* of both resistivity and hyper-resistivity in the nonlinear Hall-MHD regime. This surprising result, which was first obtained by Biskamp *et al.*,[17] can be related to the quadratic nature of the whistler wave (which mediates magnetic reconnection in the Hall-MHD regime).[12,17,20]

Figure 12 shows the scaling of the peak magnetic reconnection rate, $J_{\max}$, with the wall perturbation amplitude, Ξ_0, in the linear/nonlinear Hall-MHD regime. It is clear from the figure that the criterion for the plasma response to enter the nonlinear regime is that the *resistive* contribution to the reconnection rate should exceed unity. In other words, the perturbed current density in the reconnecting region should become comparable to the local equilibrium current density. In the linear regime, we obtain the expected $J_{\max}\sim\Xi_0^1$ scaling. On the other hand, in the nonlinear regime the reconnection rate starts to increase much more rapidly with the wall perturbation amplitude. Indeed, the figure suggests a $J_{\max}\sim\Xi_0^2$ scaling in the nonlinear regime.

Figure 13 shows the scaling of the peak magnetic reconnection rate, $J_{\max}$, with the collisionless ion skin depth, d_i, in the linear/nonlinear Hall-MHD regime. It can be seen that for $(d_i)_{\rm crit}\ll d_i\ll 1$ the rate of increase of the reconnection rate with d_i seems to be significantly stronger in the nonlinear regime ($J_{\max}\gtrsim 1$) than in the linear regime ($J_{\max}\lesssim 1$). Indeed, the figure suggests a $J_{\max}\sim d_i^{3/2}$ scaling in the nonlinear regime, as opposed to the $J_{\max}\sim d_i^1$ scaling seen in the linear regime.

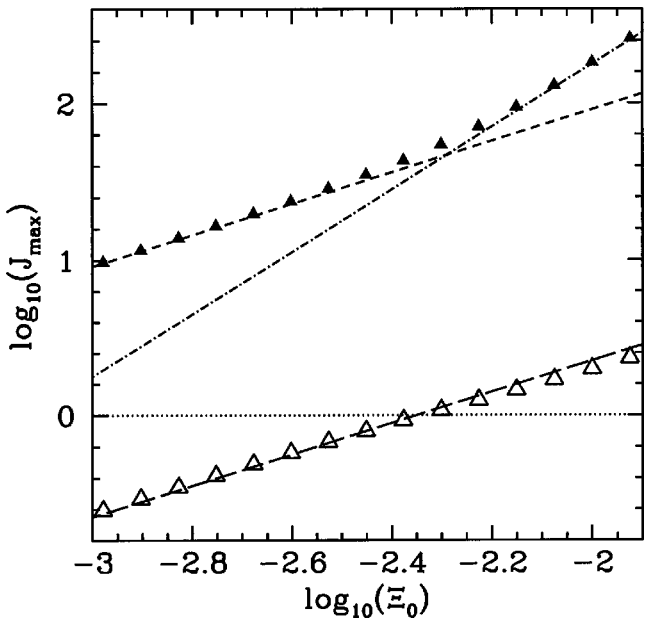

FIG. 12. Scaling of the peak magnetic reconnection rate, $J_{\max}$, with the perturbation amplitude, Ξ_0, in the linear/nonlinear Hall-MHD regime. Calculations performed with $L=8.0$, $\tau=1.0$, $\eta=10^{-6}$, $\mu_i=10^{-7}$, $\nu=2.5\times10^{-9}$, and $d_i=1.0$. The solid data points show the total reconnection rate. The open data points show the resistive contribution to the reconnection rate. The long- and short-dashed lines are fits to $J_{\max}\propto\Xi_0^1$. The dotted–dashed line is a fit to $J_{\max}\propto\Xi_0^2$.

IV. SUMMARY AND CONCLUSIONS

We have performed a comprehensive numerical study of the scaling of forced magnetic reconnection (in the absence of a guide field) in the so-called Taylor problem using a 2-D, incompressible, nonlinear Hall-MHD code. To be more exact, we have concentrated on the scaling of the *peak* instantaneous magnetic reconnection rate, $R_{\max}=(d\Psi/dt)_{\max}$, where Ψ is the reconnected magnetic flux. This metric is easily obtained from our simulations and captures the essence of the reconnection process—for instance, in the nonlinear MHD regime we are able to reproduce the classic Sweet–Parker scaling just by studying the variation of $R_{\max}$ with resistivity, η, and perturbation amplitude, Ξ_0 (see Sec. III D). Moreover, as can be seen from Fig. 1, the reconnected flux after a fixed time (since the imposition of the perturbation) increases with $R_{\max}$. Finally, $R_{\max}$ is directly proportional to the peak electric field that develops in the reconnecting region. Since it is this electric field that generates the majority of the accelerated particles that are the most important product of magnetic reconnection in astrophysical and space contexts, it makes sense to use $R_{\max}$ as a reconnection metric. Generally speaking, the inclusion of the Hall term in the plasma Ohm's law is found to *greatly accelerate* the rate of magnetic reconnection.[16,17]

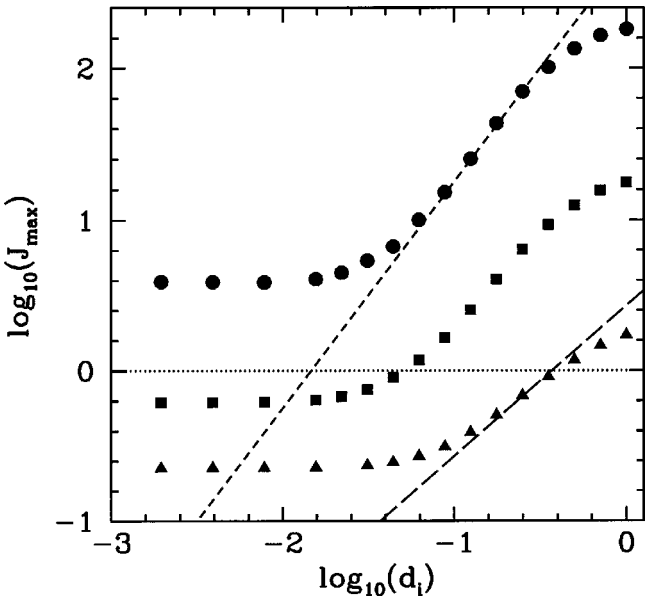

FIG. 13. Scaling of the peak magnetic reconnection rate, $J_{\max}$, with the collisionless ion skin depth, d_i, in the linear/nonlinear Hall-MHD regime. Calculations performed with $L=8.0$, $\tau=1.0$, $\mu_i=\eta/10$, $\nu=2.5\times10^{-9}$, and $\Xi_0=10^{-2}$. The triangular data points correspond to $\eta=10^{-4}$. The square data points correspond to $\eta=10^{-5}$. The circular data points correspond to $\eta=10^{-6}$. The long-dashed line is a fit to $J_{\max}\propto d_i^1$. The short-dashed line is a fit to $J_{\max}\propto d_i^{3/2}$.

Our simulations are performed in the absence of a guide field: i.e., zero equilibrium z-directed magnetic field. However, the addition of a small guide field, $B_0\hat{\mathbf{z}}$, where $B_0\ll1$ (in normalized units), would not modify any of the results reported in this paper.

In the *linear* regime (see Sec. III C), our simulations reproduce the Hahm–Kulsrud scaling[7] $R_{\max}\sim\eta^{2/3}\Xi_0$ in the conventional MHD limit. In the Hall-MHD limit, we obtain the new scaling $R_{\max}\sim d_i\eta^{1/3}\Xi_0$, where d_i is the collisionless ion skin depth. Note that this scaling breaks down as d_i approaches the system size. The critical value of d_i above which conventional MHD goes over to Hall-MHD is found to scale as $(d_i)_{\rm crit}\sim\eta^{1/3}$. Since the resistive layer width at peak reconnection rate scales as $\delta\sim\eta^{1/3}$, it is evident that conventional MHD breaks down when d_i exceeds the resistive layer width. We observe that the resistive layer width decreases as d_i increases in the Hall-MHD limit.

In the *nonlinear* regime, our simulations reproduce the Sweet–Parker scaling[18,19] $R_{\max}\sim\eta^{1/2}\Xi_0^{3/2}$ in the conventional MHD limit (see Sec. III D). In the Hall-MHD limit, we obtain the new scaling $R_{\max}\sim d_i^{3/2}\Xi_0^2$ (see Sec. III E). Again, this scaling breaks down as d_i approaches the system size. We also confirm the result obtained in Ref. 8 that the plasma response enters the nonlinear regime when the current density perturbation in the reconnecting region becomes as large as the local equilibrium current density [i.e., when $J_{\max}\equiv\eta^{-1}R_{\max}$ (or, to be more exact, the resistive component of $J_{\max}$) exceeds unity].

Note that in the nonlinear Hall-MHD limit, the peak reconnection rate is *independent* of resistivity (and hyperresistivity). In other words, the peak reconnection rate does not depend on the mechanism by which electron flux freezing is broken in the reconnecting region. This surprising result has been obtained in previous studies of Hall-MHD reconnection, and can be accounted for in terms of the quadratic nature of the whistler wave dispersion relation (note that in Hall MHD, the whistler wave controls electron motion on length scales below d_i).[12,17,20] Of course, in the limit as η (and ν) tends to zero, this η-independent scaling of

the reconnection rate must eventually break down, since it implies an X-point current density that diverges as η^{-1}. However, this limiting mechanism (which is probably electron inertia[26]) is not captured by the Hall-MHD equations.

Some previous studies have proposed that in the nonlinear Hall-MHD limit the reconnection rate is a ''universal constant'' that corresponds to a inflow velocity of about 0.1 Alfvén velocities.[12,24] We have been unable to confirm this hypothesis. However, the aforementioned studies were performed using plasmas in which the width of the equilibrium current sheet was typically *less* than d_i. Our investigation was performed in the opposite limit. In fact, in our investigation the reconnection rate in the nonlinear Hall-MHD limit is found to *vary strongly* with both the collisionless ion skin depth, d_i, and the perturbation amplitude, Ξ_0. This result is consistent with the results of a recent study by Wang *et al.*[25] (except that we cannot reproduce the exact d_i scaling reported by Wang *et al.*). Another recent study by Matthaeus *et al.*[27] has reproduced the $d_i^{3/2}$ scaling reported in this paper.

The Taylor problem, in which the plasma is subject to a fixed amplitude external perturbation, differs significantly from the so-called ''inflow'' forced reconnection problem in which the plasma is (effectively) subject to an external perturbation whose amplitude is constantly increasing in time. In the inflow problem, the phenomenon of *flux pile-up* (which does not occur in the Taylor problem) can greatly accelerate the Sweet–Parker reconnection rate.[28] Indeed, under certain circumstances the rate becomes independent of η. In the inflow problem, the inclusion of the Hall term in the plasma Ohm's law can actually *decrease* the rate of magnetic reconnection.[29] Recent studies of reconnection driven by the coalescence instability show that this problem is more closely related to the inflow problem than the Taylor problem.[30]

ACKNOWLEDGMENTS

The author gratefully acknowledges helpful discussions with Paul Watson, Jim Drake, Amitava Bhattacharjee, Luis Chacon, and Franco Porcelli during the preparation of this paper.

This research was funded by the U.S. Department of Energy under Contract No. DE-FG05-96ER-54346 as well as via Cooperative Agreement No. DE-FC02-01ER54652 under the auspices of the program for Scientific Discovery through Advanced Computing.

[1] F. L. Waelbroeck, Phys. Fluids B **1**, 2372 (1989).
[2] K. Shibata, Adv. Space Res. **17**, 9 (1996).
[3] D. N. Baker, J. Geophys. Res. **101**, 12975 (1996).
[4] D. Biskamp, Phys. Fluids **29**, 1520 (1986).
[5] B. Coppi, G. Laval, and R. Pellat, Phys. Rev. Lett. **16**, 1207 (1966).
[6] M. Ottaviani and F. Porcelli, Phys. Rev. Lett. **71**, 3802 (1993).
[7] T. S. Hahm and R. M. Kulsrud, Phys. Fluids **28**, 2412 (1985).
[8] R. Fitzpatrick, Phys. Plasmas **10**, 1782 (2003).
[9] B. U. O. Sonnerup, in *Solar System Plasma Physics*, edited by L. J. Lanzerotti, C. F. Kennel, and E. N. Parker (North-Holland, Amsterdam, 1979), Vol. 3, p. 46.
[10] S. I. Braginskii, in *Reviews of Plasma Physics* (Consultants Bureau, New York, 1965), Vol. 1, p. 205.
[11] J. Birn, J. F. Drake, M. A. Shay, B. N. Rogers, R. E. Denton, M. Hesse, M. Kuznetsova, Z. W. Ma, A. Bhattacharjee, A. Otto, and P. L. Pritchett, J. Geophys. Res. **106**, 3715 (2001).
[12] D. Biskamp, E. Schwarz, and J. F. Drake, Phys. Plasmas **4**, 1002 (1997).
[13] M. A. Shay, J. F. Drake, and B. N. Rogers, J. Geophys. Res. **106**, 3759 (2001).
[14] D. S. Harned and Z. Mikic, J. Comput. Phys. **83**, 1 (1989).
[15] H. P. Furth, J. Killeen, and M. N. Rosenbluth, Phys. Fluids **6**, 459 (1963).
[16] M. E. Mandt, R. E. Denton, and J. F. Drake, Geophys. Res. Lett. **21**, 73 (1994).
[17] D. Biskamp, E. Schwarz, and J. F. Drake, Phys. Rev. Lett. **75**, 3850 (1995).
[18] P. A. Sweet, *Electromagnetic Phenomena in Cosmical Physics* (Cambridge University Press, New York, 1958).
[19] E. N. Parker, J. Geophys. Res. **62**, 509 (1957).
[20] M. A. Shay and J. F. Drake, Geophys. Res. Lett. **25**, 3759 (1998).
[21] H. E. Petschek, in *AAS/NASA Symposium on the Physics of Solar Flares*, edited by W. N. Hess (NASA, Washington, DC, 1964), p. 425.
[22] T. Terasawa, Geophys. Res. Lett. **10**, 475 (1983).
[23] X. Wang and A. Bhattacharjee, Phys. Fluids B **4**, 1795 (1992).
[24] M. A. Shay, J. F. Drake, B. N. Rogers, and R. E. Denton, Geophys. Res. Lett. **26**, 2163 (1999).
[25] X. Wang, A. Bhattacharjee, and Z. W. Ma, Phys. Rev. Lett. **87**, 265003 (2001).
[26] F. Porcelli, D. Borgogno, F. Califano, D. Grasso, M. Ottaviani, and F. Pegoraro, Plasma Phys. Controlled Fusion **44**, B389 (2002).
[27] W. H. Matthaeus (private communication, 2003).
[28] I. J. D. Craig and P. G. Watson, Astrophys. J. **516**, 924 (1999).
[29] I. J. D. Craig, J. Heerikhuisen, and P. G. Watson, Phys. Plasmas **10**, 3120 (2003).
[30] J. C. Dorelli, Phys. Plasmas **10**, 3309 (2003).